Electronic Supplementary Information

Magneto-responsive deformable coating with lubricant self-replenishment towards on-demand scale repellence

Danna Liu,[ab†] Jiexin Li,[ab†] Ran Zhao,[ab] Yingbo Li,[ab] Li Dong,[c] Yang Wang,[ab] Weizhe Gao,[ab] Xiaosong Deng,[ab] and Jingxin Meng*[ab]

[a] Laboratory of Bio-inspired Smart Interface Science, Technical Institute of Physics and Chemistry, Chinese Academy of Sciences, Beijing 100190, P. R. China. Email：mengjx628@mail.ipc.ac.cn

[b] University of Chinese Academy of Sciences, Beijing 100049, P. R. China.

[c] Department of Orthodontics, Peking University School and Hospital of Stomatology, Beijing 100081, P. R. China

* Corresponding authors

† These authors have contributed equally to this work

Contents:

1. Supplementary Notes

1.1 Materials

Polydimethylsiloxane (PDMS, Sylgard 184) was purchased from Dow Corning (USA). n-Hexane, Calcium chloride anhydrous (96%), nanometer calcium carbonate (50 nm), sodium sulfate anhydrous (99%), sodium chloride, rhodamine B and paraffin liquid were purchased from Macklin Biochemical Technology Co., Ltd. (China). Co (99.9% metals basis, ≤ 500 nm), silicone oil PMX-200 (10 mPa.s, neat) and sodium hydroxide were purchased from Aladdin Chemical (China). Ethylenediamine tetraacetic acid disodium salt (EDTA-Na_2, AR) was purchased from Sinopharm Chemical Reagent Co., Ltd. (China). SiO_2 nanoparticles (R972 were purchased from Lijie Chemical Co., Ltd (China). Commercial polyurethane sponge (thickness: 3 mm) was purchased from Yunzongcheng New Materials Manufacturer (China). Krytox 100 was purchased from DuPont (USA). All aqueous solutions were prepared using deionized water (Milli-Q system, 18.2 MΩ·cm, Bedford, MA, USA). All reagents were used directly without further purification.

1.2 Characterization

Surface morphology was observed using an environmental scanning electron microscope (ESEM) (FEI, Quanta FEG 250, USA). Magnetic field strength was measured using a Gauss meter (Tunkia, TD8620, China). Energy dispersive spectrometry (EDS) analysis was conducted to observe the distribution of magnetic particles within the PDMS matrix. Room-temperature hysteresis loops of MRDC samples with varying Co contents were measured using a vibrating sample magnetometer (VSM, Lakeshore 7404, Lake Shore, USA) The replenishing process was recorded using a Sony camera (FDR-AXP55). The surface tension and interfacial tension were measured using the pendant drop method. The deposited scale was quantified using Inductively Coupled Plasma Atomic Emission Spectroscopy (ICP-AES, Varian 710-OES, USA). The contact angle of air and water was measured using an SCA-20 instrument at room temperature (Data-physics, Germany). The adhesion force between the lubricant and surfaces was evaluated using a high-sensitivity microelectromechanical balance system (DCAT 11, Data-physics, Germany). A Laser scanning confocal microscope (OLS-4500, Olympus, Japan) was employed to map the 3D surface topography and determine the average surface roughness (Ra) of the samples.

1.3 Theoretical criterion and energy calculation for stable lubricating film formation

According to the lubricating film stability conditions, three overall system energies need to be compared: E_1 (lubricant in mineral solution wetting the surface), E_2 (mineral solution in air wetting the surface), and E_3 (lubricant in air wetting the surface). A stable lubricating film can theoretically form if the following conditions are satisfied: $\Delta E_1 = E_2 - E_1 > 0$ and $\Delta E_2 = E_2 - E_3 > 0$.[1]

Here, ΔE_1 and ΔE_2 can be expressed as:

$$\Delta E_1 = R(\gamma_{l_2}\cos\theta_{l_2} - \gamma_{l_1}\cos\theta_{l_1}) - \gamma_{l_1 l_2} \quad \text{(S1)}$$

$$\Delta E_2 = R(\gamma_{l_2}\cos\theta_{l_2} - \gamma_{l_1}\cos\theta_{l_1}) + \gamma_{l_1} - \gamma_{l_2} \quad \text{(S2)}$$

where R represents the roughness coefficient of the MDL with a rough structure (R = 2.02), and the roughness coefficient is the ratio of the actual area to the projected area. The symbols γ_{l_1}, γ_{l_2} and $\gamma_{l_1 l_2}$ represent the interfacial energy of the mineral solution in air (l_1), the interfacial energy of the lubricant (l_2) in air, and the interfacial energy between the mineral solution and the lubricant, respectively. The γ_{l_1} is 72.4 mJ/m^2 and θ_{l_1} is 142.2°. The energy relationships between three common lubricants (*i.e.*, Krytox 100, silicone oil, and liquid paraffin) and saturated $CaSO_4$ solution are compared.

By using the hanging drop method and a contact angle meter, various contact angle values and a series of interfacial energy values were obtained. Through these values, ΔE_1 and ΔE_2 can be calculated. The relevant values and calculation results are listed in Table S1.

1.4 The calculation of Gibbs energy barrier of scale nucleus

The value of ΔG was determined by $f(m,x)$ is expressed as

$$\Delta G = kf(m,x) = \frac{1}{2}\left\{1 + \left(\frac{1 - mx}{g}\right)^3 + x^3\left[2 - 3\left(\frac{x - m}{g}\right) + \left(\frac{x - m}{g}\right)^3\right] + 3mx^2\left(\frac{x - m}{g} - 1\right)\right\} \quad \text{(S3)}$$

where

$$g = \left(1 + x^2 - 2mx\right)^{1/2} \quad \text{(S4)}$$

And k is a constant for scale crystal nucleation. $x = R/r_c$, R represents roughness radius of the surface, r_c represents the critical nucleus size. We used the approach developed by Ghasemi *et al.* to determine the value of m.

The first case is MRDC with stable lubricant film. According to Young's equation, θ_1 can be written as

$$\gamma_{nk} = \gamma_{sk} - \gamma_{ns}\cos\theta_1 \quad \text{(S5)}$$

while the θ_2 can be written as

$$\gamma_{nk} = \gamma_{ns} - \gamma_{sk}\cos\theta_2 \quad \text{(S6)}$$

where n, s, k represents scale nucleus, salt solution and Krytox 100, respectively. By subtraction of these equations, m_1 can be calculated as

$$m_1 = \cos\theta_1 = \frac{\gamma_{sk}}{\gamma_{ns}}\left(1 + \cos\theta_2\right) - 1 \quad \text{(S7)}$$

In contrast, after depletion of lubricant film, the scale nucleus was directly contact with the rough surface of MRDC. In this case, θ_3 can be calculated as

$$\gamma_{nm} = \gamma_{sm} - \gamma_{ns}\cos\theta_3 \quad \text{(S8)}$$

Where $m_2$and θ_3. The interfacial tension of MRDC-D-salt solution (γ_{sm}) can be calculated using Young's equation

$$\gamma_{sm} = \gamma_{ma} - \gamma_{sa}\cos\theta_4 \quad \text{(S9)}$$

where γ_{ma} and γ_{sa} represent the interfacial tension of the rough surface of MRDC-D-air and salt solution-air, respectively. θ_4 is the contact angle of a $CaSO_4$ solution droplet on the rough surface

of MRDC-D in air. The interfacial tension of scale nucleus-rough surface of MRDC-D can be calculated as reported[2]

$$\gamma_{nm} = \gamma_n + \gamma_m - 2\sqrt{\gamma_n \gamma_m} \quad \text{(S10)}$$

where γ_n and γ_m represent the surface energy of the scale nucleus and the rough surface of MRDC-D, respectively. Therefore, m_2 ($m_2 = \cos\theta_3$) can be calculated by combination of equation (S8), (S9) and (S10).

The PDMS surface were also directly contacted with the scale nucleus. Therefore, the value of m_3 can be calculated the same way as m_2. The above-mentioned interfacial tension was summarized in Table S2. Having all these parameters, we found that the value of m_1, m_2 and m_3 were -0.91, 0.55, 0.36, respectively.

1.5. The calculation of the interfacial energies

Both of γ_{cs} and γ_{sm} can be calculated using Young's equation

$$\gamma_{cs} = \gamma_{ca} - \gamma_{sa} \cos\theta_5 \quad \text{(S11)}$$

According to a previous research, the value of the contact angle of a $CaSO_4$ solution droplet on the $CaSO_4$ substrate was 0°.[3] Then the interfacial energy between scale crystal and rough surface of MRDC (γ_{cm}) can be expressed as[4]

$$\gamma_{cm} = \left(\sqrt{\gamma_c^{LW}} - \sqrt{\gamma_m^{LW}}\right)^2 + 2\left(\sqrt{\gamma_c^+ \gamma_c^-} + \sqrt{\gamma_m^+ \gamma_m^-} - \sqrt{\gamma_c^+ \gamma_m^-} - \sqrt{\gamma_m^+ \gamma_c^-}\right) \quad \text{(S12)}$$

where γ^+, γ^- and γ^{LW} represent the polar components from the Lewis acid and base sites and the nonpolar component of surface energy, respectively. The contact angles of three standard liquids (water, glycerol and n-hexadecane) are required to calculate γ_m, the related results were also shown in Table S3. Therefore, we can obtain the value of γ_{cs}, γ_{sm} and $\gamma_{cm}$was -12.7 mJ/m^2, 58.4 and 18.0 mJ/m^2, respectively. The adhesion work between PDMS surface and scale crystal (W_{cp}^a) can also be calculated the same way as above and the value of γ_{sp} and $\gamma_{cp}$was 44.3 mJ/m^2 and 3.46 mJ/m^2, respectively.

2. Supplementary Figures

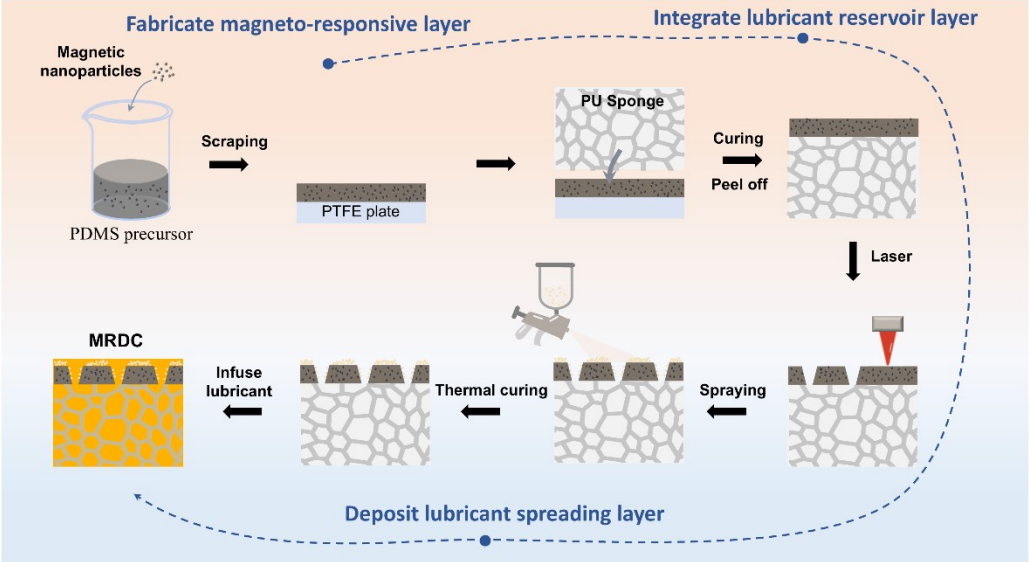

Fig. S1. Schematic illustration depicting the fabrication process of MRDC.

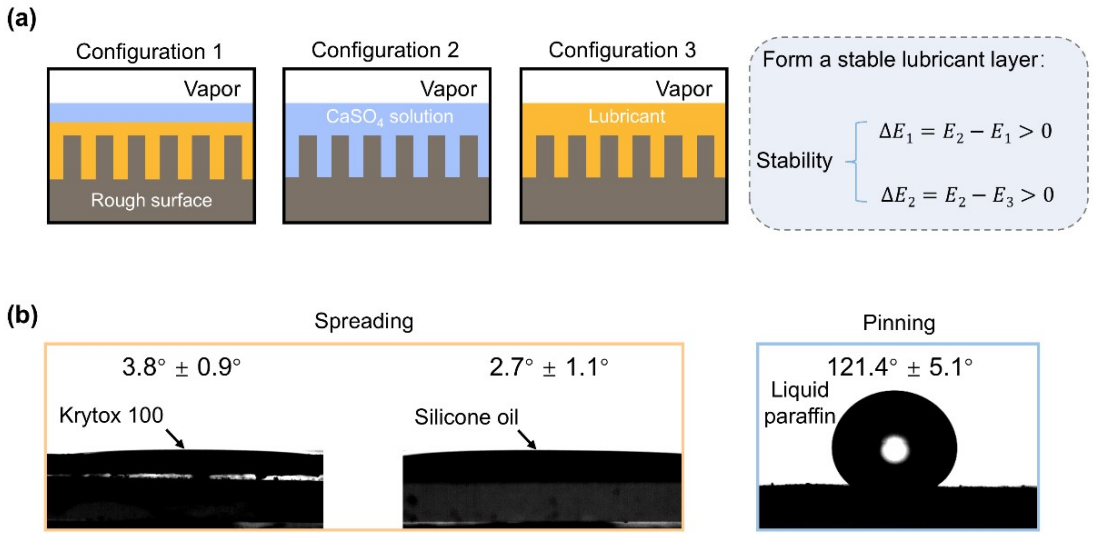

Fig. S2. Selection of lubricants. (a) Schematic diagrams of the working conditions required to maintain a stable lubricating film. (b) Contact angles of Krytox 100, silicone oil, and liquid paraffin measured on the MRDC surface.

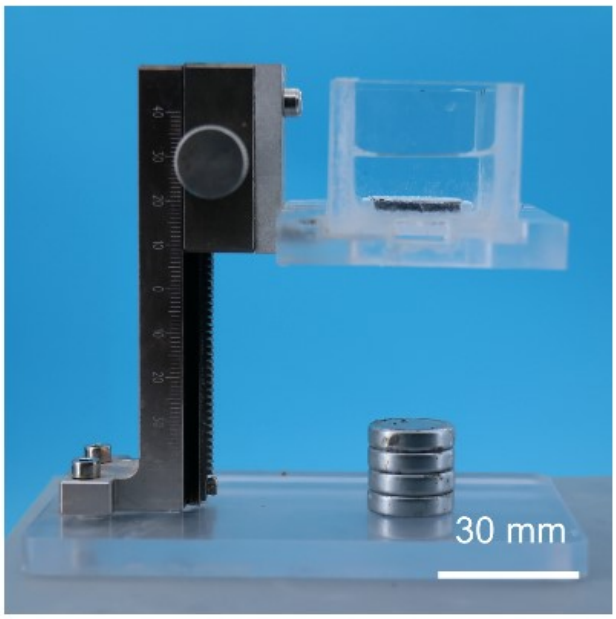

Fig. S3. Photograph of the experimental set-up for adjusting the magnetic field strength.

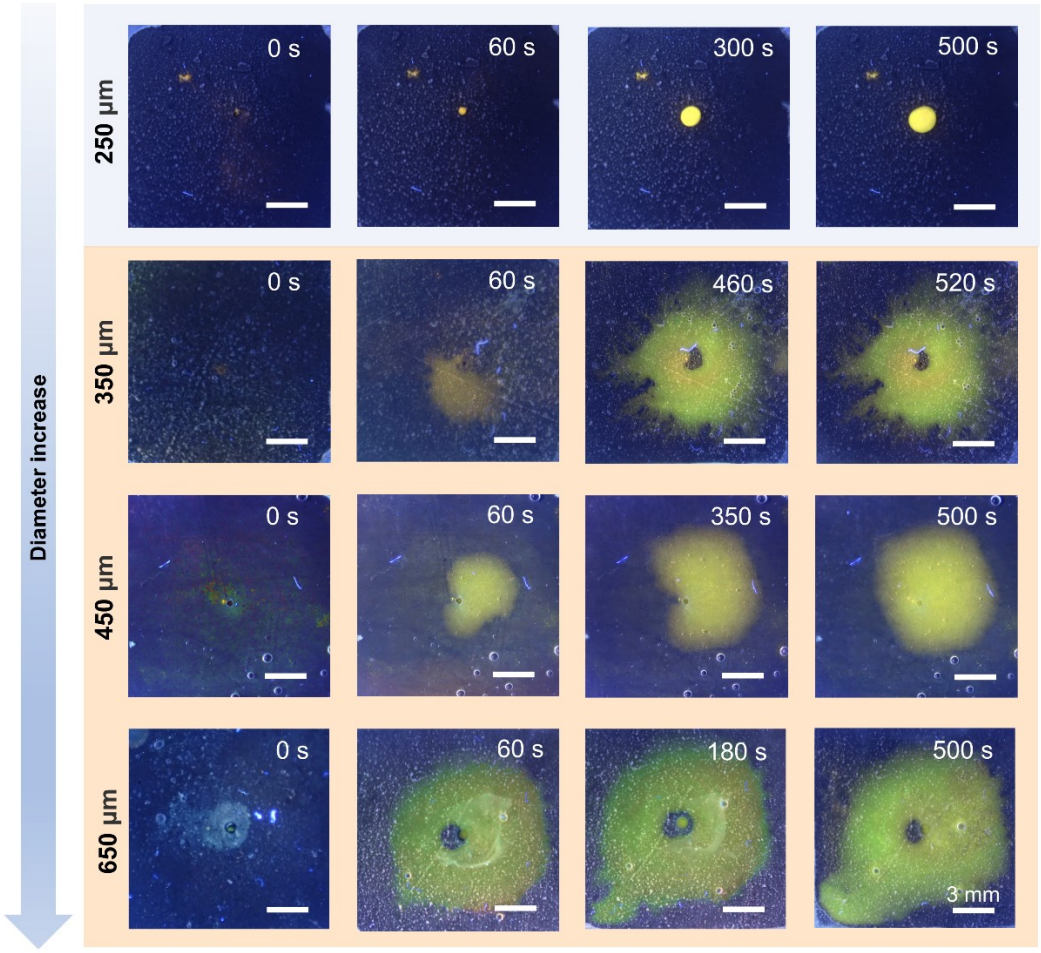

Fig. S4. The effect of pore diameters on lubricant spreading area.

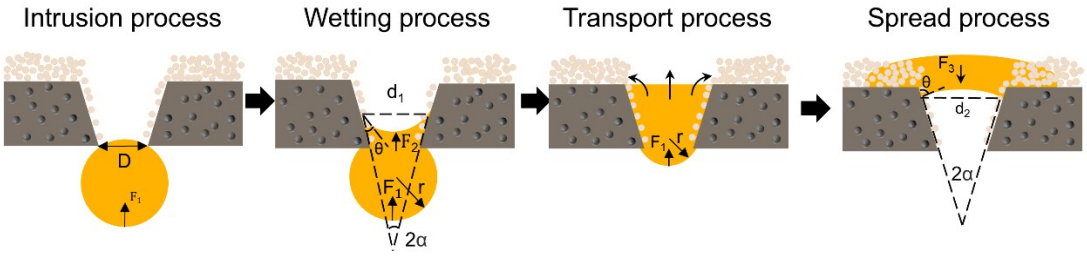

Fig. S5. Schematic illustration of lubricant transport and replenishment processes. Lubricant replenishment from the LRL to the upper LSL involves intrusion, wetting, transport, and spreading processes. F_1, F_2, and F_3 denote the surface tension, capillary force, and drag force, respectively.

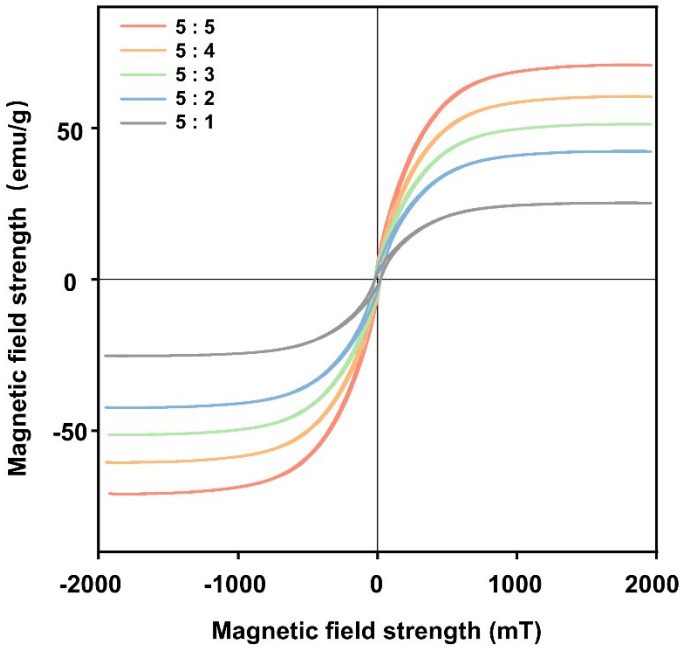

Fig. S6. Magnetization as a function of magnetic field strength for the MRDC with the mass ratios of PDMS:Co varying from 5:1 to 5:5.

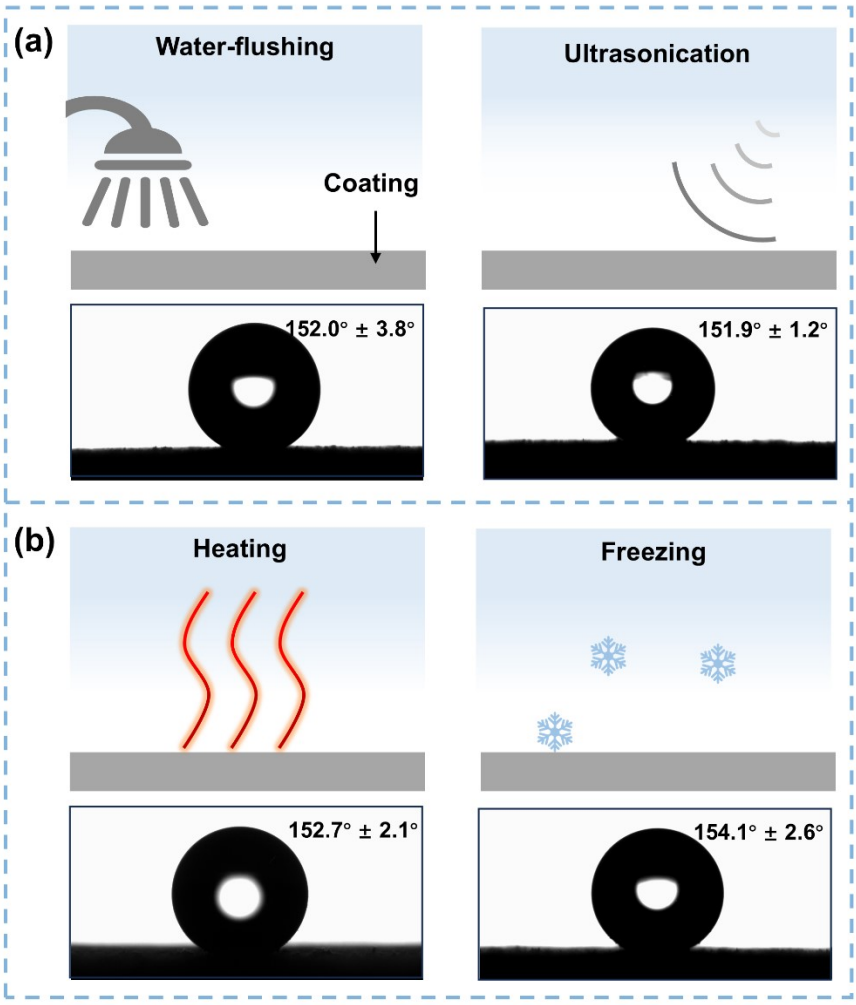

Fig. S7. Schematic illustrations of stability tests and corresponding WCA of lubricant-free MRDC. (a) Mechanical stability evaluation *via* water flushing and underwater ultrasonication. (b) Thermal stability evaluation *via* hot water immersion and freezing.

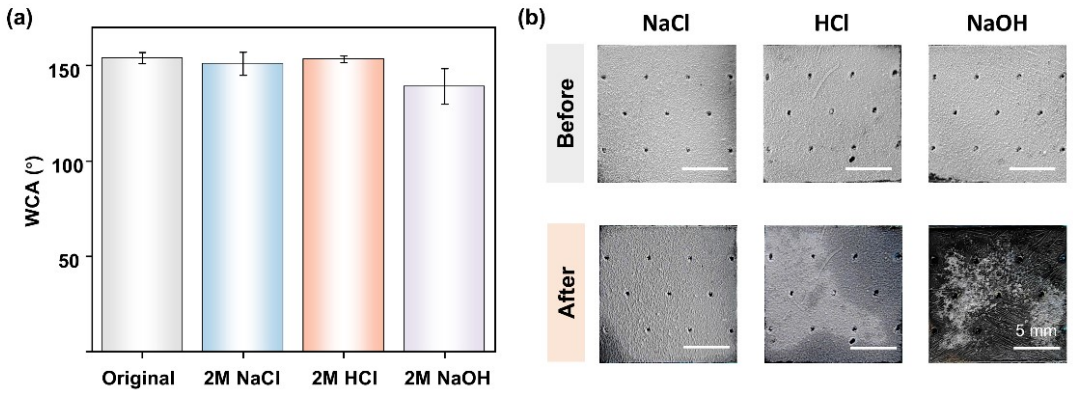

Fig. S8. The corrosion resistance performance of the lubricant-free MRDC. (a) The WCA of lubricant-free MRDC original and after immersion in acidic, alkaline, and saline solution for 12h. (b) Optical image before and after immersion in acidic, alkaline, and saline solution.

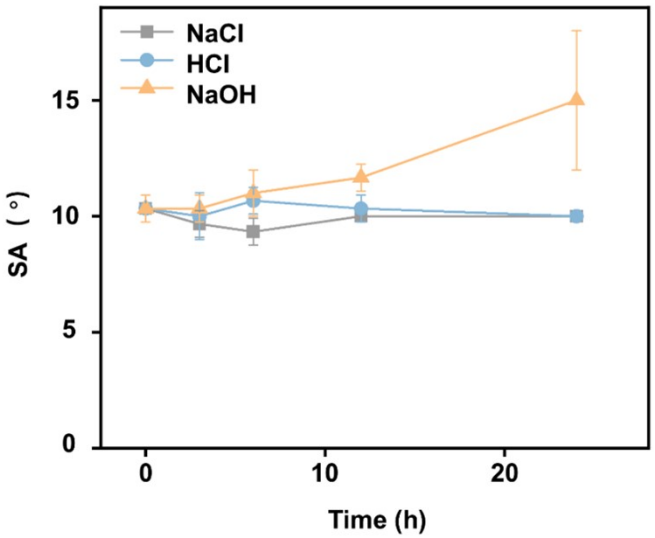

Fig. S9. SAs of the MRDC after immersion in acidic (2 M), alkaline (2 M), and saline solution (2 M) for different times.

3. Supplementary Tables

Table S1. Comparison of surface energy of different liquid systems

Lubricant	γ_{l_2} (mJ/m^2)	$\gamma_{l_1 l_2}$ (mJ/m^2)	θ_{l_1} (°)	θ_{l_2} (°)	ΔE_1 (mJ/m^2)	ΔE_2 (mJ/m^2)
Krytox 100	16.3	53.0	142.2	3.8	95.4	92.4
Silicone oil	17.8	34.1	142.2	2.2	117.4	96.9
Paraffin liquid	28.5	42.2	142.2	121.4	43.3	41.7

Table S2. Summary of interfacial energy across different interfaces

Interface	Interfacial energy	Value (mJ/m^2)	Data source
$CaSO_4$ solution-Krytox 100	γ_{sk}	53	Experiment
$CaSO_4$ solution-MRDC	γ_{sm}	58.4	Equation (S9)
Scale nucleus-$CaSO_4$ solution	γ_{ns}	95	Reference[5]
Scale nucleus-MRDC	γ_{nm}	6.36	Equation (S10)
MRDC-air	γ_{ma}	27.3	Experiment
Scale nucleus-PDMS	γ_{np}	10.1	Equation (S10)
$CaSO_4$ solution-PDMS	γ_{sp}	44.3	Equation (S9)
Scale crystal-$CaSO_4$ solution	γ_{cs}	-12.7	Equation (S11)
Scale crystal-MRDC	γ_{cm}	18.0	Equation (S12)
Scale crystal-PDMS	γ_{cp}	3.46	Equation (S12)

Table S3. Summary of surface energy of materials

Material	γ (mJ/m^2)	γ^{LW} (mJ/m^2)	γ^+ (mJ/m^2)	γ^- (mJ/m^2)
$CaSO_4$	59.7	41.1	1.3	65.5
MRDC-D	27.7	27.7	0	0.61
PDMS	20.7	20.7	0	0

Note: γ denotes surface tension. γ^{LW} is the Lifshitz-van der Waals component of surface energy. γ^+ and γ^- are the polar components from the Lewis acid and Lewis base sites, respectively.

4. References

1. T.-S. Wong, S. H. Kang, S. K. Y. Tang, E. J. Smythe, B. D. Hatton, A. Grinthal and J. Aizenberg, *Nature*, 2011, **477**, 443-447.
2. J. Restolho, J. L. Mata and B. Saramago, *J. Colloid Interface Sci.*, 2009, **340**, 82-86.
3. H. Fan, X. Song, Y. Xu and J. Yu, *Appl. Surf. Sci.*, 2019, **478**, 594-600.
4. C. J. Van Oss, M. K. Chaudhury and R. J. Good, *Chem. Rev.*, 1988, **88**, 927-941.
5. A. Masoudi, P. Irajizad, N. Farokhnia, V. Kashyap and H. Ghasemi, *ACS Appl. Mater. Interfaces*, 2017, **9**, 21025-21033.